ISTS-2017-d-159／ISSFD-2017-159

EQUULEUS Mission Analysis: Design of the Transfer Phase

By Kenta OSHIMA,[1)] Stefano CAMPAGNOLA,[2)] Chit Hong YAM,[3)] Yuki KAYAMA,[4)] Yasuhiro KAWAKATSU,[5)] Naoya OZAKI,[6)] Quentin VERSPIEREN,[6)] Kota KAKIHARA,[6)] Kenshiro OGURI,[6)] and Ryu FUNASE [6)]

[1)]*Department of Applied Mechanics and Aerospace Engineering, Waseda University, Tokyo, Japan*
[2)]*Jet Propulsion Laboratory, California Institute of Technology, CA, USA*
[3)]*ispace inc., Tokyo, Japan*
[4)]*Department of Advanced Energy, The University of Tokyo, Tokyo, Japan*
[5)]*Institute of Space and Astronautical Science, JAXA, Sagamihara, Japan*
[6)]*Department of Aeronautics and Astronautics, The University of Tokyo, Tokyo, Japan*

This paper highlights the design of the transfer phase of EQUULEUS (EQUilibriUm Lunar-Earth point 6U Spacecraft), which aims to reach and stay at the Earth-Moon L_2 libration point orbit to observe the far-side of the Moon. Since EQUULEUS is a piggyback CubeSat, there are original challenges that past missions have not faced so far. We develop a systematic trajectory design approach to tackle the difficulties. The trajectory is a nearly-ballistic low-energy transfer to a quasi-periodic halo orbit around Earth-Moon L_2 using lunar flybys and solar perturbation.

Key Words: EQUULEUS, Trajectory Design, Lunar Flyby, Solar Perturbation, Optimization

1. Introduction

Scheduled in 2018, Exploration Mission-1 (EM-1) will launch the Orion Multi-Purpose Crew Vehicle with 13 CubeSats via the NASA's new SLS rocket. EQUULEUS (EQUilibriUm Lunar-Earth point 6U Spacecraft, Fig. 1) is one of the selected CubeSats, proposed and being developed by JAXA and The University of Tokyo. EQUULEUS aims to reach a lunar libration point orbit around the Lagrange point L_2 to observe the far side of the Moon.[1), 2), 3)]

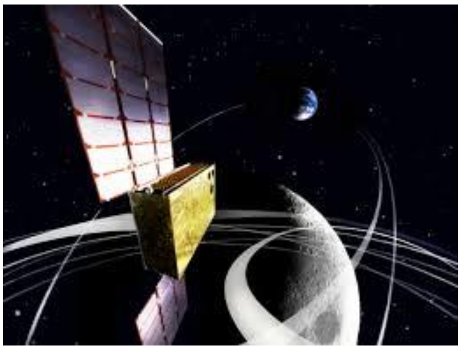

Fig. 1. An artist's concept of EQUULEUS.

In order to reach the lunar L_2 libration point orbit, EQUULEUS will use lunar flybys (LFBs) and solar perturbation to achieve low-energy transfer.[4)] Other CubeSats in EM-1 such as Lunar IceCube[5)], Lunar Polar Hydrogen Mapper[6)], Lunar Flashlight[7)], and OMOTENASHI[8)] will transfer to the Moon, and Lunar Icecube and Lunar Polar Hydrogen Mapper also plan to use luni-solar perturbation.

In past missions, HITEN[9)] and GRAIL[10)] realized low-energy transfers to the Moon, and ARTEMIS[11)] reached the Earth-Moon L_2 libration point orbit by using LFBs and solar perturbation. Many studies investigated the class of low-energy transfer in terms of the gravitational capture mechanism[4), 12)], the dynamical systems theory[13)], and global search strategies [14), 15), 16)].

Comparing with these past missions and researches, EQUULEUS has its original challenges because it is a piggyback, CubeSat. The first challenge is the constrained launch condition of SLS, which targets low-altitude LFB making a ballistic trajectory escape from the Earth-Moon system. Therefore, EQUULEUS must change the 1^{st} LFB condition by its thruster to return to the Earth-Moon system. The demonstration of the controllability of a CubeSat under luni-solar perturbation is one of the main objectives. A robust and flexible framework of designing transfer trajectories is necessary to deal with constrained initial conditions especially near launch.

The second challenge is the limited $\triangle v$ budget, approximately 80 [m/s] for the whole mission, including trajectory correction maneuvers (TCMs) and clean up maneuvers (CUMs) before and after LFBs, and stationkeeping $\triangle v$ on the science orbit[21)]. Ideally, the transfer phase is nearly ballistic for arbitrary launch conditions.

The third challenge is the critical execution of $\triangle v_1$ to achieve the desirable 1^{st} LFB condition. Currently, EQUULEUS plans to start $\triangle v_1$ 1 day after the separation from SLS and finish the execution of $\triangle v_1$, orbit determination, and TCMs before the 1^{st} LFB, which occurs approximately 6 days after the separation. Considering the limited thrust capability, 3 [mN] at most, the operation before the 1^{st} FLB could be tight[2)] and therefore it is important to reduce $\triangle v_1$ as much as possible.

This paper presents our current strategy to tackle these challenges. We develop a systematic method for designing transfer trajectories from the separation from SLS to capture into a lunar L_2 quasi-periodic halo orbit in a high-fidelity model. Error analyses including TCM, CUM, and Monte Carlo simulation are out of scope of this paper. The present analysis uses the launch condition that the epoch of the separation is 2018 OCT 07 15:39 (UTC) given by NASA.

The reminder of this paper is organized as follows. Section 2 introduces the basic concept of low-energy transfer. Section 3 highlights our approach of designing transfer trajectories. Section 4 shows results of computing transfer trajectories.

2. Low-Energy Transfer

Belbruno and Miller[4)] found low-energy transfer to the Moon, which has remarkable benefits such as lower △v and a wider launch window as compared with the high-energy Hohmann-type transfer. The mechanism of the low-energy lunar transfer is based on the use of the solar tidal force[12)], which accelerates a trajectory, pumps up its perigee, and reduces v_∞ with respect to the Moon if an apogee is placed in the 2nd or 4th quadrant around the Earth and vice versa.

Fig. 2 shows an example of low-energy transfer to the Moon[16)], which places its apogee in the 2nd quadrant to reduce v_∞. The trajectory uses LFB to save Earth departure △v and exploits solar perturbation to reduce lunar insertion △v.

Since the original trajectory of Orion encounters the Moon with high v_∞, EQUULEUS needs to reduce v_∞ by using solar perturbation to achieve low-energy capture into the Earth-Moon L_2 quasi-periodic halo orbit.

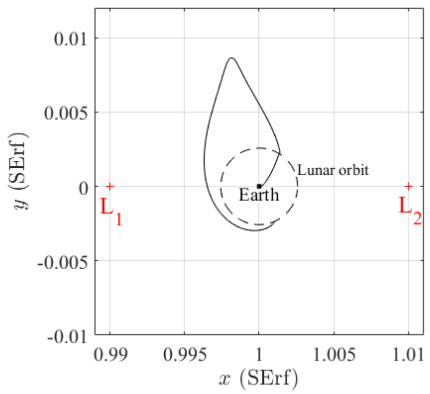

Fig. 2. An example of low-energy transfer to the Moon computed in Oshima et al.[16)] The trajectory is shown in the non-dimensional Sun-Earth rotating frame.

3. Trajectory Design Approach

Fig. 3 shows a flowchart of our trajectory design approach for EQUULEUS. The following sections highlight each process with some backgrounds.

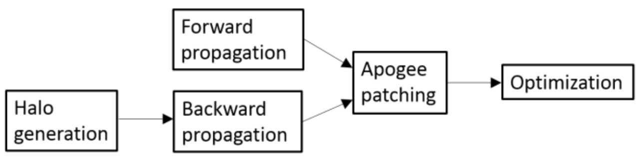

Fig. 3. A flowchart of the trajectory design approach for EQUULEUS.

3.1. Halo Generation Process

This process computes multi-revolutional quasi-periodic orbits around lunar L_2. Periodic halo orbits in the Earth-Moon circular restricted three-body problem (CR3BP) are optimized along the wide range of epoch in the full-ephemeris model by using the optimization software jTOP.[17)]

Note that periodic orbits in autonomous systems such as the CR3BP cannot persist when including time-dependent perturbations except for special resonant cases. Instead, natural dynamical substitutes of periodic orbits in non-autonomous systems such as the ephemeris model are quasi-periodic orbits.[18), 19), 20)]

See Oguri et al.[21)] for details of the computation of quasi-periodic halo orbits and the analysis of stationkeeping △v for EQUULEUS. Fig. 4 shows eight families of quasi-periodic halo orbits computed in Oguri et al.[21)] In this paper, we use the quasi-periodic halo orbits of the epoch from 2019 JAN 01 to 2019 MAY 31, but those of a different time range could generate more families of solutions.

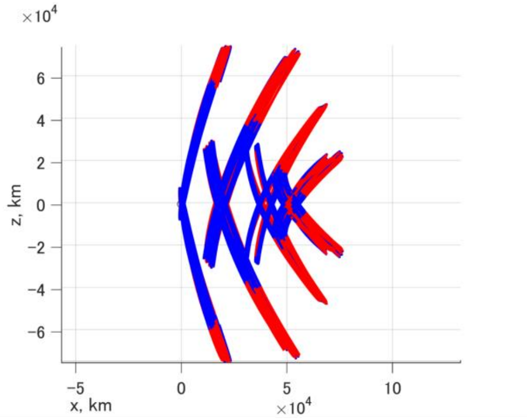

Fig. 4. Families of quasi-periodic halo orbits.[21)]

3.2. Forward Propagation Process

This process propagates trajectories forward in time from the separation, currently including gravitational effects of the Sun, Earth, and Moon as point masses, and saves time and states at apogees. After 1 day from the separation, we apply impulsive △v_1 to change the 1st LFB condition. The computation is three-dimensional grid search in terms of the magnitude and angles of △v_1. Since the execution of △v_1 is critical as denoted in Section 1, we set the lower bound of the magnitude of △v_1 such that some trajectories can come back to the Earth-Moon system after the 1st apogee even though most of them escape. In this analysis, the lower bound is 2 [m/s] and the upper bound is 6 [m/s].

Fig. 5 shows an example of a trajectory propagated forward in time with △v_1=2 [m/s]. Since △v_1 is small, the trajectory comes back to the Earth-Moon system after the high 1st apogee distance. We confirm that the large values of z (> 770,000 [km]) at 1st apogees of △v_1=2 [m/s] make it difficult to patch with backward legs from the quasi-periodic halo orbits (see Section 3.3), i.e., larger △v_1 is necessary to design trajectories for the conditions of the current analysis.

Fig. 6 shows values of (a) x, (b) y, and (c) z at apogees in the Earth-centered J2000 frame in terms of ephemeris time as the result of the grid search. From these figures, we extract time and position of the 1st apogee as

$$\begin{aligned} &5.95\times10^{8}\le t\le 5.995\times10^{8}\ \ [\mathrm{s}],\\ &-12.5\times10^{5}\le x\le -5\times10^{5}\ \ [\mathrm{km}],\\ &-3.8\times10^{5}\le y\le 16\times10^{5}\ \ [\mathrm{km}],\\ &0\le z\le 12\times10^{5}\ \ [\mathrm{km}]. \end{aligned} \tag{1}$$

This condition of the 1st apogee is used to restrict the data to patch at 1st apogees (see Section 3.4).

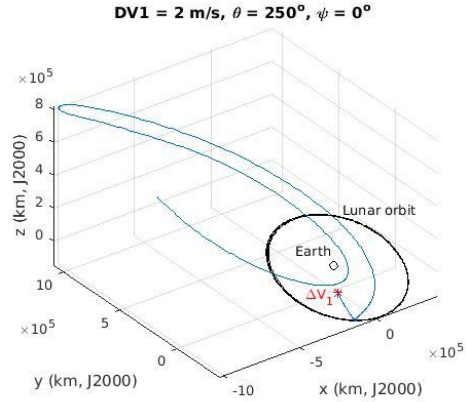

Fig. 5. An example of a trajectory propagated forward in time with △v_1=2 [m/s] in the Earth-centered J2000 frame.

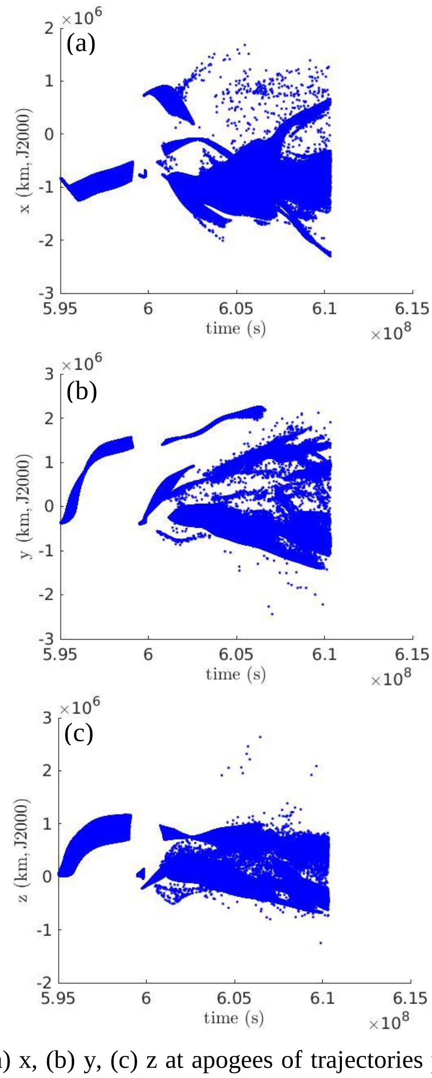

Fig. 6. (a) x, (b) y, (c) z at apogees of trajectories propagated forward in time in the Earth-centered J2000 frame in terms of ephemeris time.

3.3. Backward Propagation Process

This process propagates trajectories backward in time from quasi-periodic halo orbits, currently including gravitational effects of the Sun, Earth, and Moon as point masses, and saves time and states at apogees. In order to escape from the quasi-periodic halo orbits efficiently, we apply small △v to the minimum stretching direction.

The minimum stretching direction $\delta\boldsymbol{x_i}$ is defined by using the state transition matrix (STM) Φ as

$$\min_{\delta\boldsymbol{x_i}}\left\|\delta\boldsymbol{x_f}\right\|, \tag{2}$$

where

$$\left\|\delta\boldsymbol{x_f}\right\| = \sqrt{\delta\boldsymbol{x_i}^T\Phi^T\Phi\delta\boldsymbol{x_i}}. \tag{3}$$

From Eqs. (2) and (3), the minimum stretching direction is the eigenvector associated to the minimum eigenvalue of the Cauchy-Green tensor $\mathrm{C}=\Phi^T\Phi$.

The minimum stretching direction of the Cauchy-Green tensor can be regarded as an extension of the eigenvector of the stable direction of the Monodromy matrix in autonomous systems to non-autonomous systems, which was used in the computation of Lagrangian coherent structures[22), 23)] and an analysis of the low-energy gravitational capture of BepiColombo to Mercury.[24)]

Fig. 7 shows trajectories propagated backward in time by applying small △v (=0.1[m/s]) to minimum stretching directions from one quasi-periodic halo orbit. The trajectories can be regarded as an extension of stable manifolds in autonomous systems to non-autonomous systems. EQUULEUS aims to get on one of these time-dependent analogues of stable manifolds[23)] to be captured into a quasi-periodic halo orbit with small insertion △v.

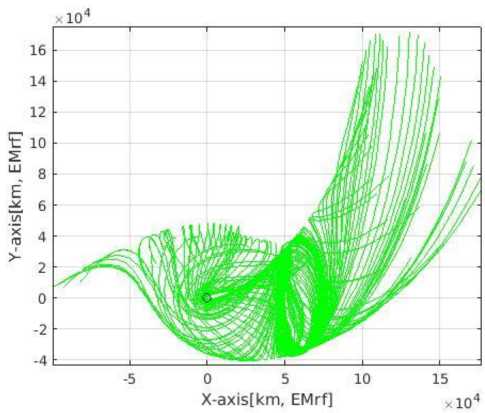

Fig. 7. Trajectories propagated backward in time by applying small velocity perturbation to minimum stretching directions from a quasi-periodic halo orbit around lunar L_2 in the Moon-centered Earth-Moon rotating frame.

3.4. Apogee Patching Process

This process patches forward (Section 3.2) and backward (Section 3.3) legs at 1st apogees. We only use the data at apogees of the backward propagation that satisfy Eq. (1). We use the MATLAB function knnsearch to find k-nearest neighbors in terms of time and position at apogees, and extract pairs such that differences of time and distance between apogees are less than prescribed tolerances (TOLE.t and TOLE.rmag). We sort these pairs in ascending order in terms of the magnitude of the difference of velocity (discontinuity

△v). If the differences of time and distance between apogees are small enough, discontinuity △v could be a good criterion to measure the quality of initial guesses, which is ideally equal to △v subtracting $△v_1$ from total △v after optimization.

Fig. 8 shows forward ($△v_1$=6 [m/s], blue) and backward (red) states at apogees, displayed with those satisfying tolerances TOLE.t=0.025[days] and TOLE.rmag=25,000[km] (green for forward and black for backward) in (a) x-y, (b) x-z, (c) vx-vy, (d) vx-vz planes in the Earth-centered J2000 frame.

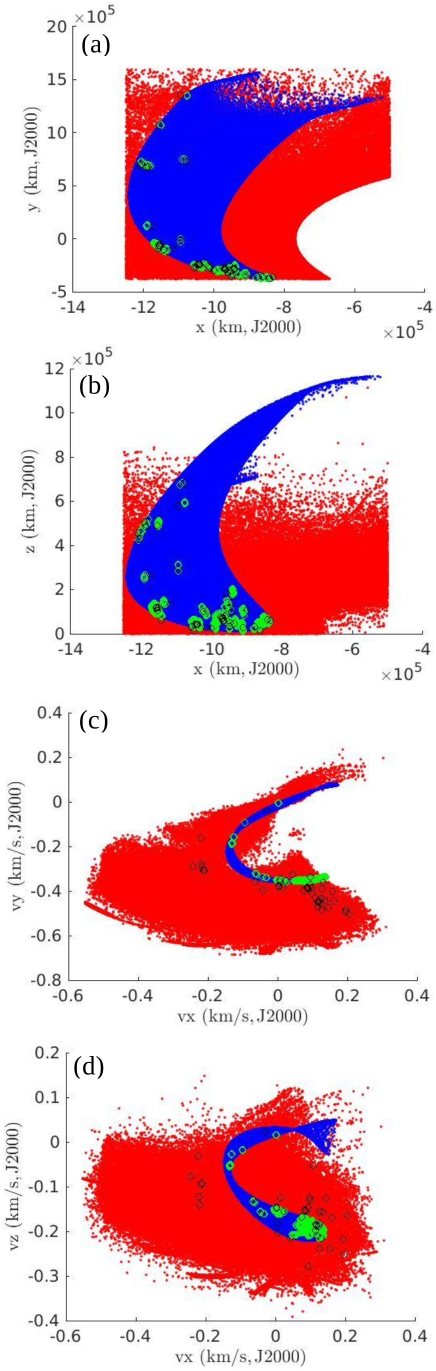

Fig. 8. Forward ($△v_1$=6 [m/s], blue) and backward (red) states at apogees, displayed with those satisfying the tolerances TOLE.t=0.025[days] and TOLE.rmag=25,000[km] (green for forward and black for backward) in (a) x-y, (b) x-z, (c) vx-vy, (d) vx-vz planes in the Earth-centered J2000 frame.

We note that our previous method patched forward and backward legs at perilunes.[2), 25), 26), 27)] However, the current method of patching at apogees has the following advantages as compared with the previous method. Firstly, the current method enables easier design of transfer trajectories using LFB once, i.e., only the 1st LFB, because the states at 1st LFBs of forward propagation are similar and it is difficult to distinguish good initial guesses. Note that substantial differences arise after the 1st LFB due to the sensitivity of LFB. Greater numbers of LFBs result in larger navigation △v such as TCM and CUM, and more challenging operations. Secondary, the current method can naturally include deep space maneuver (DSM) as the velocity discontinuity at apogees in initial guess, whereas the previous method cannot without fixing $△v_1$ or adding extra dimensionality to the search space. Thirdly, it is easier to predict △v to patch forward and backward legs before optimization in the current method (see Section 4), whereas it was difficult in the previous method because states at perilunes are sensitive due to the strong gravity of the Moon[26), 27)].

3.5. Optimization Process

This module optimizes the initial guesses satisfying tolerances TOLE.t and TOLE.rmag by using the optimization software jTOP[17)], which was successfully used to design the trajectory of PROCYON[28)], the first deep-space micro-spacecraft. jTOP covers from low-fidelity to high-fidelity dynamics and both impulsive and finite thrust maneuvers. Currently, we optimize trajectories of EQUULEUS including gravitational effects of the Sun, Jupiter, Earth, and Moon as point masses, and minimize total △v by assuming impulsive maneuvers.

jTOP optimizes trajectories via the direct multiple shooting method. Fig. 9 schematically shows the patching strategy of jTOP, where arcs are propagated forward and backward in time from each phase, and additional phase is introduced in the sensitive region to improve the convergence.

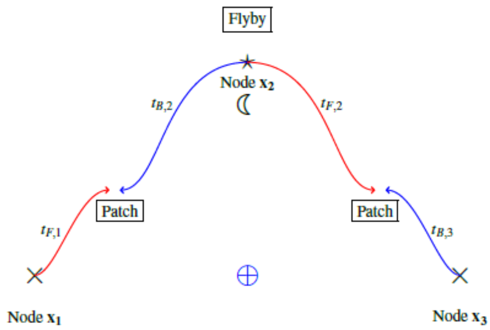

Fig. 9. A Schematic figure of the patching strategy of jTOP.

4. Results

This section presents the results of designing transfer trajectories for EQUULEUS based on the above procedures.

Fig. 10 shows the results of optimizing initial guesses of discontinuity △v < 100[m/s]. In this analysis, we only optimize one initial guess in each family, and families are classified in terms of dates of LFBs and time of flight (TOF). Fig. 10 (a) shows the values of TOF and total △v. Several families of solutions and trade-off between TOF and total $\triangle v$ are visible. Fig. 10 (b) shows $\triangle v_1$ and total $\triangle v$, which indicates that the changes of $\triangle v_1$ via the optimization are small. It is possible to put a constraint on the magnitude of $\triangle v_1$ though we did not use it in this analysis. Fig. 10 (c) shows the discontinuity $\triangle v$ at apogees of initial guesses and $\triangle v$ subtracting $\triangle v_1$ from total $\triangle v$ after optimization. There is a near-linear relationship between these values and thus $\triangle v$ is quantitatively predictable before the optimization.

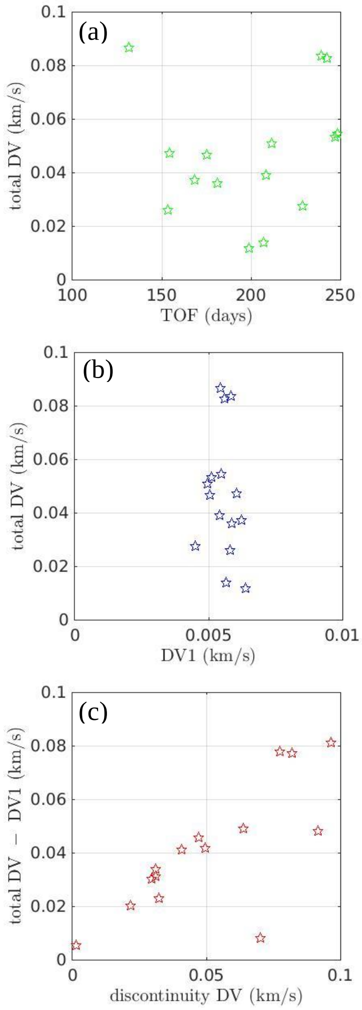

Fig. 10. (a) TOF and total $\triangle v$ of optimal solutions. (b) $\triangle v_1$ and total $\triangle v$ of optimal solutions. (c) Discontinuity $\triangle v$ of the initial guesses and $\triangle v$ subtracting $\triangle v_1$ from total $\triangle v$ after optimization.

Fig. 11 (a), (b) show the transfer trajectory of the optimal solution with total $\triangle v$=11.5 [m/s], $\triangle v_1$=6.4 [m/s], TOF=199 [days] in the (a) Sun-Earth and (b) Earth-Moon rotating frames. The red and blue arcs represent the initial guess, and the green and magenta arcs represent the optimal solution. Since the discontinuity at the apogee of the initial guess was small, the trajectories of the initial guess and the optimal solution nearly overlap. The trajectory reaches a quasi-periodic halo orbit by using LFB only once, which could save navigation $\triangle v$ and relax complexity of the operation.

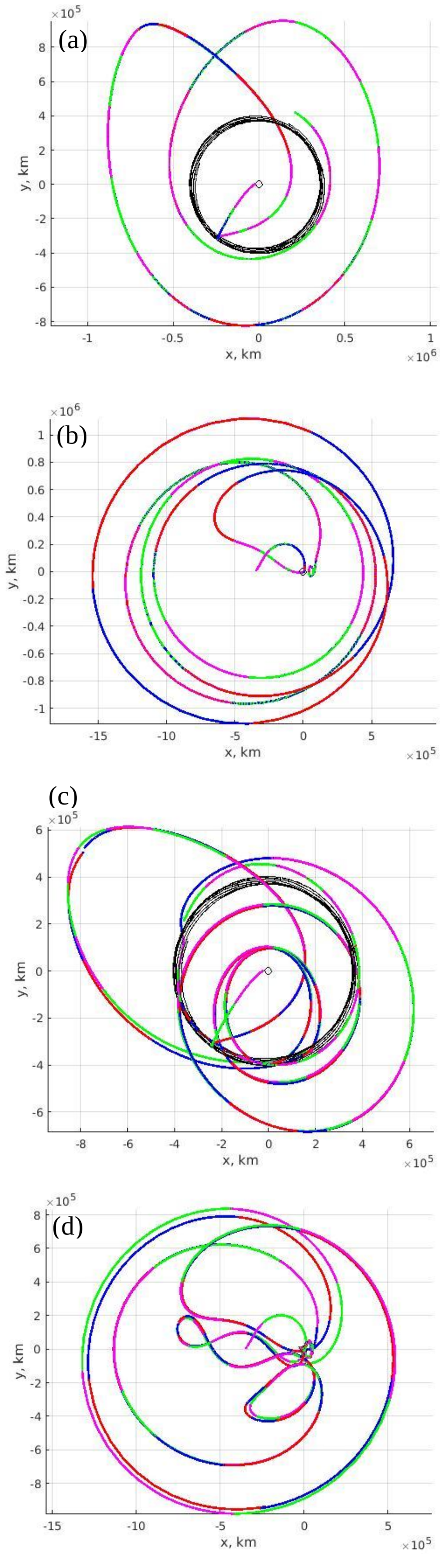

Fig. 11. Optimal transfer trajectories with (a), (b) total $\triangle v$=11.5 [m/s], $\triangle v_1$=6.4 [m/s], TOF=199 [days], and (c), (d) total $\triangle v$=13.7 [m/s], $\triangle v_1$=5.7 [m/s], TOF=207 [days] in the (a), (c) Sun-Earth and (b), (d) Earth-Moon rotating frames, respectively. The red and blue arcs represent the initial guess, and the green and magenta arcs represent the optimal solution.

Fig. 11 (c), (d) show the transfer trajectory of the optimal solution with total $\triangle v$=13.7 [m/s], $\triangle v_1$=5.7 [m/s], TOF=207 [days] in the (c) Sun-Earth and (d) Earth-Moon rotating frames. This solution uses multiple LFBs, but results in smaller $\triangle v_1$. Multiple LFBs may be useful to reduce $\triangle v_1$, and there could be tread-off between numbers of LFBs and the magnitude of $\triangle v_1$.

5. Conclusion

This paper presented the trajectory design approach of EQUULEUS for low-energy transfers to the Earth-Moon L_2 quasi-periodic halo orbit. Our method could systematically compute families of transfers using lunar flybys and solar perturbation. We showed that total $\triangle v$ and $\triangle v_1$ are predictable before optimization, which is a favorable feature for an efficient search.

References

1) Funase, R., Ozaki, N., Nakajima, S., Oguri, K., Miyoshi, K., Campagnola, S., Koizumi, H., Kobayashi, Y., Ito, T., Kudo, T., Koshiro, Y., Nomura, S., Wachi, A., Tomooka, M., Yoshikawa, I., Yano, H., Abe, S. and Hashimoto, T.: Mission to Earth-Moon Lagrange Point by a 6U CubeSat: EQUULEUS, 31th International Symposium on Space Technology and Science, Ehime, Japan, 2017-f-043, 2017.
2) Campagnola, S., Ozaki, N., Oguri, K., Verspieren, Q., Kakihara, K., Yanagida, K., Funase, R., Yam, C. H., Ferella, L., Yamaguchi, T., Kawakatsu, Y. and Yárnoz, D. G.: Mission Analysis for EQUULEUS, JAXA's Earth-Moon Libration Orbit Cubesat, 67th International Astronautical Congress, Guadalajara, Mexico, IAC-16-B4.8.1, 2016.
3) Campagnola, S., Ozaki, N., Hernando, J., Oshima, K., Yamaguchi, T., Ikenaga, T., Yam, C. H., Oguri, K., Kakihara, K., Takahashi, S., Ozawa, Y., Ferella, L., Funase, R. and Hashimoto, T.: Mission Analysis for EQUULEUS and OMOTENASHI, 31th International Symposium on Space Technology and Science, Ehime, Japan, 2017-f-044, 2017.
4) Belbruno, E. and Miller, J.: Sun-Perturbed Earth-to-Moon Transfers with Ballistic Capture, *J. Guid. Control Dyn.,* **16** (1993), pp. 770-775.
5) Bosanac, N., Cox, A., Howell, K. C. and Folta, D. C.: Trajectory Design for a Cislunar Cubesat Leveraging Dynamical Systems Techniques: The Lunar IceCube Mission, 27th AAS/AIAA Space Flight Mechanics Meeting, San Antonio, USA, AAS 17-286, 2017.
6) Genova, A. L. and Dunham, D. W.: Trajectory Design for the Lunar Hydrogen Mapper Mission, 27th AAS/AIAA Space Flight Mechanics Meeting, San Antonio, USA, AAS 17-456, 2017.
7) Hayne, P. O., Greenhagen, B. T., Paige, D. A., Camacho, J. M., Cohen, B. A., Sellar, G. and Reiter, J.: Lunar Flashlight: Illuminating the Lunar South Pole, 47th Lunar and Planetary Science Conference, The Woodlands, USA, 2016.
8) Hashimoto, T., Yamada, T., Kikuchi, J., Otsuki, M. and Ikenaga, T.: Nano Moon Lander: OMOTENASHI, 31th International Symposium on Space Technology and Science, Ehime, Japan, 2017-f-053, 2017.
9) Uesugi, K., Matsuo, H., Kawaguchi, J. and Hayashi, T.: Japanese First Double Lunar Swingby Mission "HITEN", *Acta Astronaut.*, **25** (1991), pp. 347-355.
10) Hoffman, T. L.: GRAIL: Gravity Mapping of the Moon, IEEE Aerospace Conference, Big Sky, USA, 2017-f-053, 2009.
11) Angelopoulos, V.: The ARTEMIS Mission, *Space Sci. Rev.*, **165** (2011), pp. 3-25.
12) Kawaguchi, J., Yamakawa, H., Uesugi, T. and Matsuo, H.: On Making Use of Lunar and Solar Gravity Assists in LUNAR-A, PLANET-B Missions, *Acta Astronaut.*, **35** (1995), pp. 633-642.
13) Koon, W. S., Lo, M. W., Marsden, J. E. and Ross, S. D.: Low Energy Transfer to the Moon, *Celest. Mech. Dyn. Astr.*, **81** (2001), pp. 63-73.
14) Parker, J. S. and Anderson, R. L.: Surveying Ballistic Transfers to Low Lunar Orbit, *J. Guid. Control Dyn.*, **36** (2013), pp. 1501-1511.
15) Topputo, F.: On Optimal Two-Impulse Earth-Moon Transfers in a Four-Body Model, *Celest. Mech. Dyn. Astr.*, **117** (2013), pp. 279-313.
16) Oshima, K., Topputo, F. and Yanao, T.: Global Search for Low-Energy Transfers to the Moon with Long Transfer Time, 27th AAS/AIAA Space Flight Mechanics Meeting, San Antonio, USA, AAS 17-299, 2017.
17) Campagnola, S., Ozaki, N., Sugimoto, Y., Yam, C. H., Hongru, C., Kawabata, Y., Ogura, S., Sarli, B., Kawakatsu, Y., Funase, R. and Nakasuka, S.: Low-Thrust Trajectory Design and Operations of PROCYON, the First Deep-Space Micro-Spacecraft, 25th International Symposium on Space Flight Dynamics, Munich, Germany, 2015.
18) Gómez, G. and Mondelo, J. M.: The Dynamics around the Collinear Equilibrium Points of the RTBP, *Phys. D*, **157** (2001), pp. 283-321.
19) Campagnola, S., Lo, M. and Newton, P.: Subregions of Motion and Elliptic Halo Orbits in the Elliptic Restricted Three-Body Problem, 18th AAS/AIAA Space Flight Mechanics Meeting, Galveston, USA, AAS 08-200, 2008.
20) Dei Tos, D. A., and Topputo, F.: Trajectory Refinement of Three-Body Orbits in the Real Solar System Model, *Adv. Space Res.*, (2017).
21) Oguri, K., Kakihara, K., Campagnola, S., Ozaki, N., Oshima, K., Yamaguchi, T. and Funase, R.: EQUULEUS Mission Analysis: Design of the Science Orbit Phase, 31th International Symposium on Space Technology and Science, Ehime, Japan, 2017-d-072, 2017.
22) Haller, G.: Distinguished Material Surfaces and Coherent Structures in Three-Dimensional Fluid Flows, *Phys. D*, **149** (2001), pp. 248-277.
23) Gawlik, E. S., Marsden, J. E., Du Toit, P. C. and Campagnola, S.: Lagrangian Coherent Structures in the Planar Elliptic Restricted Three-Body Problem, *Celest. Mech. Dyn. Astr.*, **103** (2009), pp. 227-249.
24) Campagnola, S. and Lo, M.: BepiColombo Gravitational Capture and the Elliptic Restricted Three-Body Problem, 6th International Congress on Industrial and Applied Mathematics, Zurich, Switzerland, 2007.
25) Yárnoz, D. G., Yam, C. H., Campagnola, S. and Kawakatsu, Y.: Extended Tisserand-Poincaré Graph and Multiple Lunar Swingby Design with Sun Perturbation, 6th International Conference on Astrodynamics Tools and Techniques, Darmstadtium, Germany, 2016.
26) Yam, C. H., Kayama, Y., Suda, S. and Kawakatsu, Y.: Matching of Patched-Integrated Trajectories for Lunar Gravity Assists, 26th Workshop on JAXA Astrodynamics and Flight Mechanics, Sagamihara, Japan, 2016.
27) Kayama, Y., Yam, C. H., Oshima, K., Suda, S. and Kawakatsu, Y.: Matching of Patched-Hyperbolas for Lunar Gravity-Assist Trajectory Design, 31th International Symposium on Space Technology and Science, Ehime, Japan, 2017-d-024, 2017.
28) Funase, R., Inamori, T., Ikari, S., Ozaki, N., Nakajima, S., Koizumi, H., Tomiki, A., Kobayashi and Kawakatsu, Y.: One-Year Deep Space Flight Result of the World's First Full-Scale 50kg-Class Deep Space Probe PROCYON and Its Future Perspective, Small Satellite Conference, 2016.